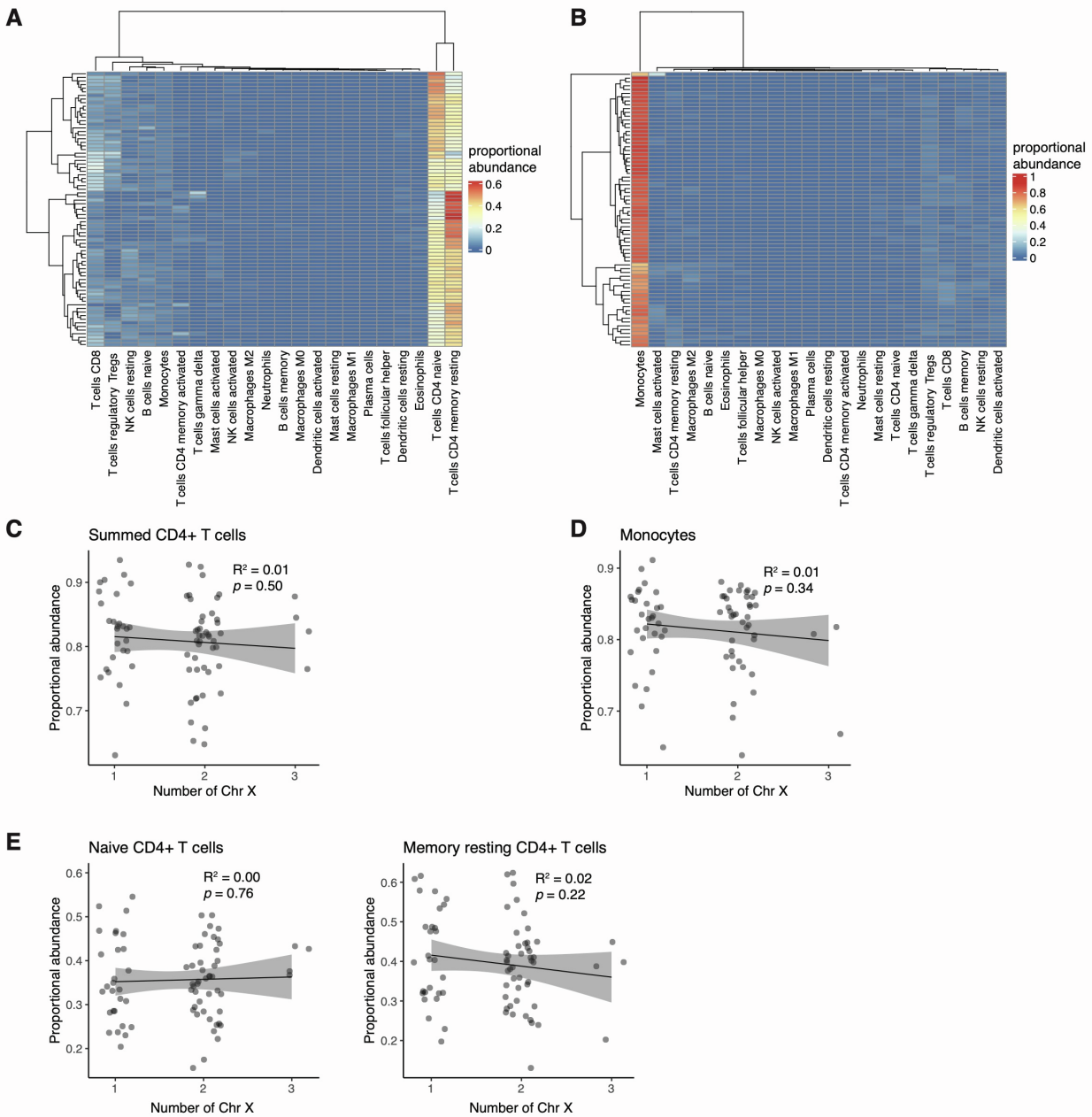


**Supplemental information**

**Stable and robust Xi and Y transcriptomes drive  
cell-type-specific autosomal and Xa responses  
*in vivo* and *in vitro* in four human cell types**

**Laura V. Blanton, Adrianna K. San Roman, Geryl Wood, Ashley Buscetta, Nicole Banks, Helen Skaletsky, Alexander K. Godfrey, Thao T. Pham, Jennifer F. Hughes, Laura G. Brown, Paul Kruszka, Angela E. Lin, Daniel L. Kastner, Maximilian Muenke, and David C. Page**

**Figure S1**



**Figure S1. Computational cell-type deconvolution confirms enrichment of CD4+ T cells and monocytes, related to Figure 1.**

(A, B) Heatmaps of estimated proportional abundances, as predicted by CIBERSORTx, for CD4+ T cell samples (A) and monocytes (B). Each row is a single sample; columns indicate cell

type identities. **(C)** Summed estimated proportional abundances of CD4+ T cells within a given sample, plotted by donor Chr X count. Linear regression statistics shown, indicating no significant change in CD4+ T cell abundance with the number of Chr X. **(D)** Estimated proportional abundances of monocyte samples, plotted by donor Chr X count. Linear regression statistics shown, indicating no significant change in monocyte abundance with the number of Chr X. **(E)** Estimated proportional abundances of naïve CD4+ T cells and memory resting CD4+ T cells. Linear regression statistics shown, indicating no significant change in CD4+ T cell abundance by Chr X count.

Figure S2

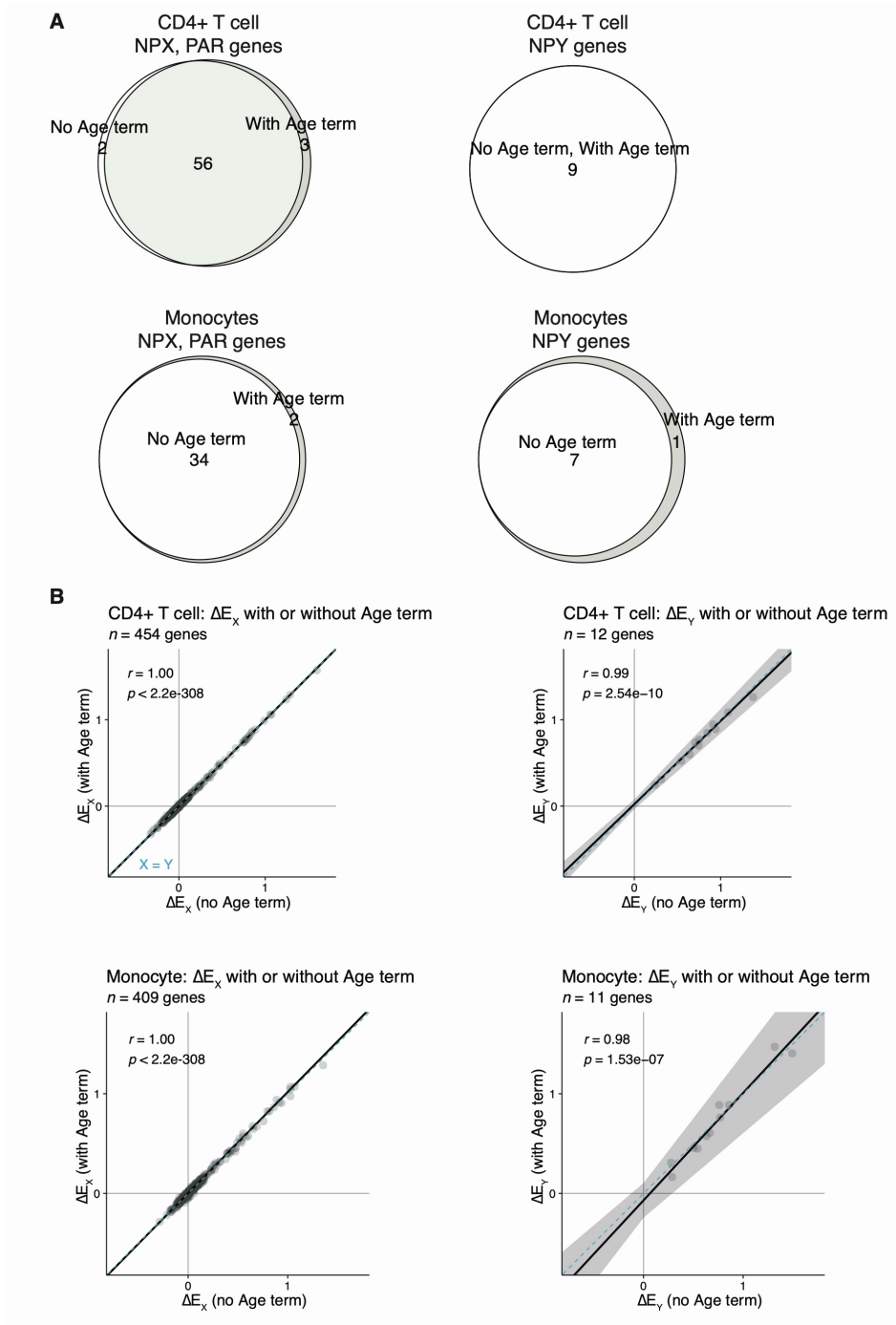
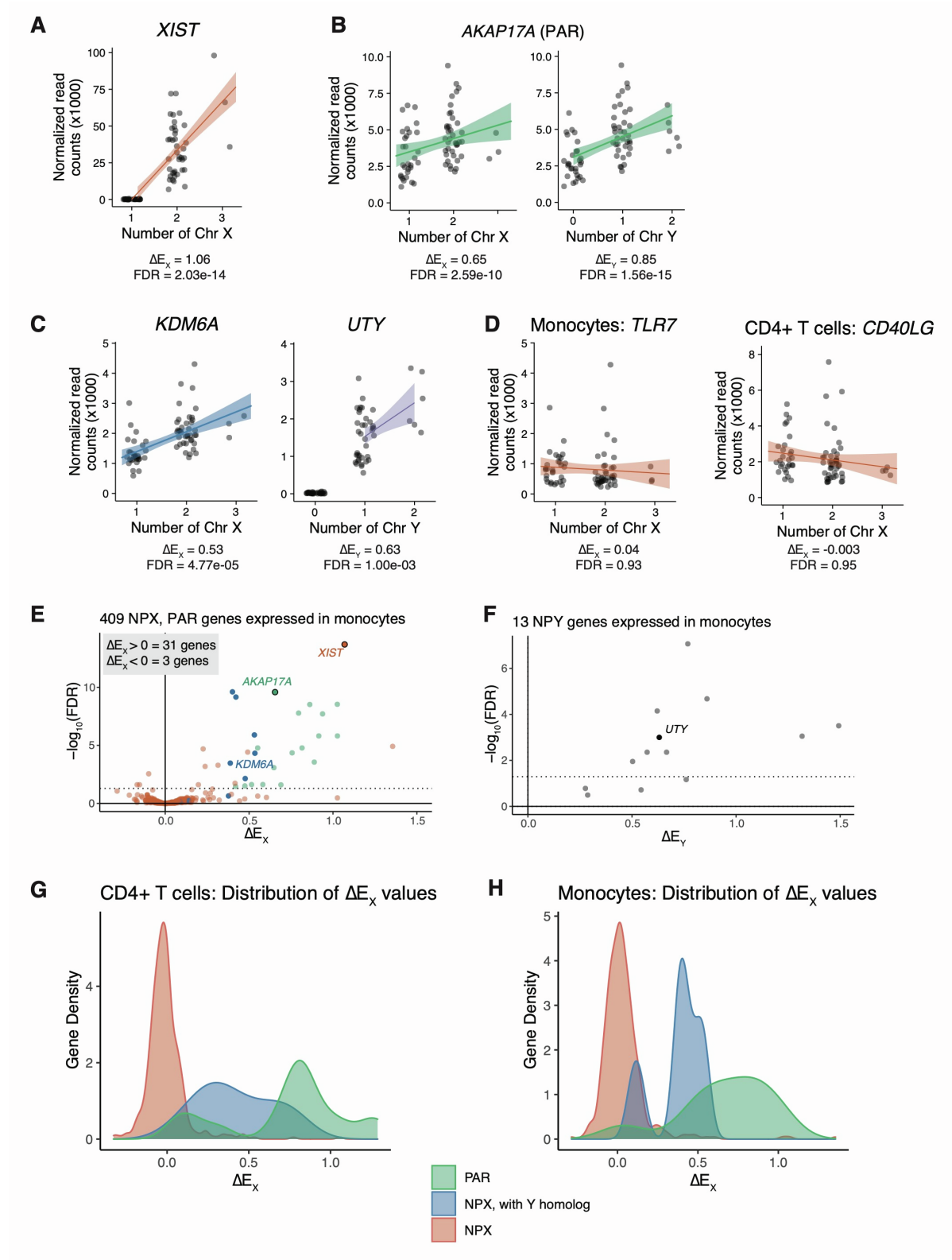


Figure S2. Inclusion of age in linear model does not impact  $\Delta E_x$  or  $\Delta E_y$ , related to Figure 1.

(A) Venn diagrams representing the number of X- or Y-chromosomal genes with significant responses to Chr X or Chr Y dosage, as indicated, with or without inclusion of age as a variable

in the linear model. **(B)** Scatter plots of  $\Delta E_X$  or  $\Delta E_Y$  values, as indicated, in CD4+ T cells and monocytes with or without inclusion of age as a variable in the linear model. Deming regression line in black with 95% confidence intervals shaded gray; blue dotted lines indicate X=Y identity line. Pearson correlation statistics are shown.

Figure S3



**Figure S3. Expression of X- and Y-chromosomal genes respond to Xi and Y dosage in monocytes, related to Figure 1.**

(A - D) Normalized read counts (x1000) by sex chromosome dosage for *XIST* (A), the PAR gene *AKAP17A* (B), the NPX-NPY homologous pair *KDM6A* and *UTY* (C), or the immune-related genes *TLR7* (in monocytes) and *CD40LG* (in CD4<sup>+</sup> T cells) (D). Regression lines with confidence intervals are shown. (E, F) Volcano plots of  $\Delta E_X$  values of all expressed NPX and PAR genes (E) or  $\Delta E_Y$  values of expressed NPY genes (F) in monocytes. Dotted horizontal lines indicate FDR = 0.05. In (A), genes are annotated by gene class: PAR genes in green, NPX genes with NPY homologs in blue, and NPX genes with no NPY homolog in orange. (G, H) Density plots showing distributions of  $\Delta E_X$  values by gene class in CD4<sup>+</sup> T cells (G) and monocytes (H).

**Figure S4**

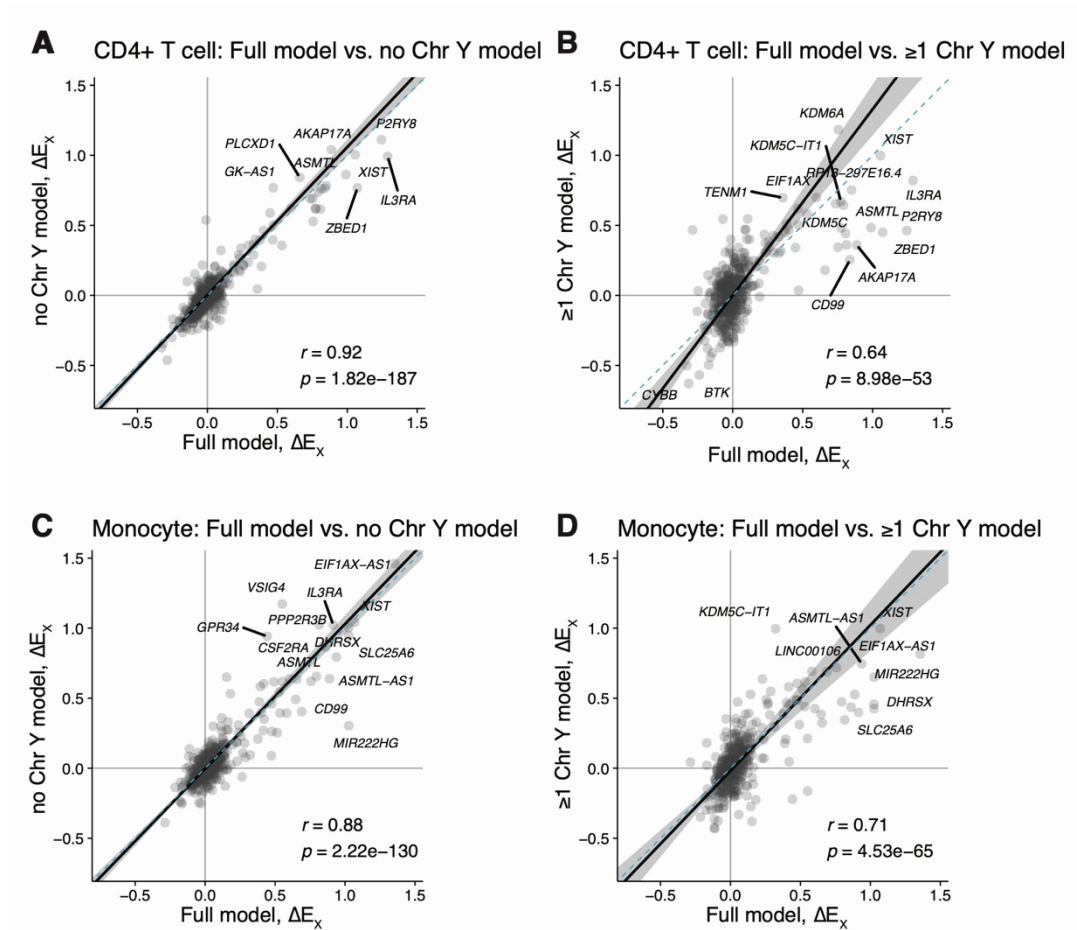


**Figure S4. Linear models built with no Chr Y or at least one Chr Y correlate with the full model containing all karyotypes, related to Figure 1.**

**(A, B)** Scatter plot of  $\Delta E_x$  values for all expressed NPX and PAR genes in CD4+ T cells, comparing effect sizes found in full model with all available karyotypes versus ‘no Chr Y’ subset model **(A)** or karyotypes with at least one Chr Y **(B)**. **(C, D)** Scatter plot of  $\Delta E_x$  values for all expressed NPX and PAR genes in monocytes, comparing effect sizes found in full model with all available karyotypes versus ‘no Chr Y’ subset model **(C)** or karyotypes with at least one Chr Y



**(D)**. Deming regression line in black with 95% confidence intervals shaded gray; blue dotted lines indicate  $X=Y$  identity line. Pearson correlation statistics are shown.

**Figure S5**

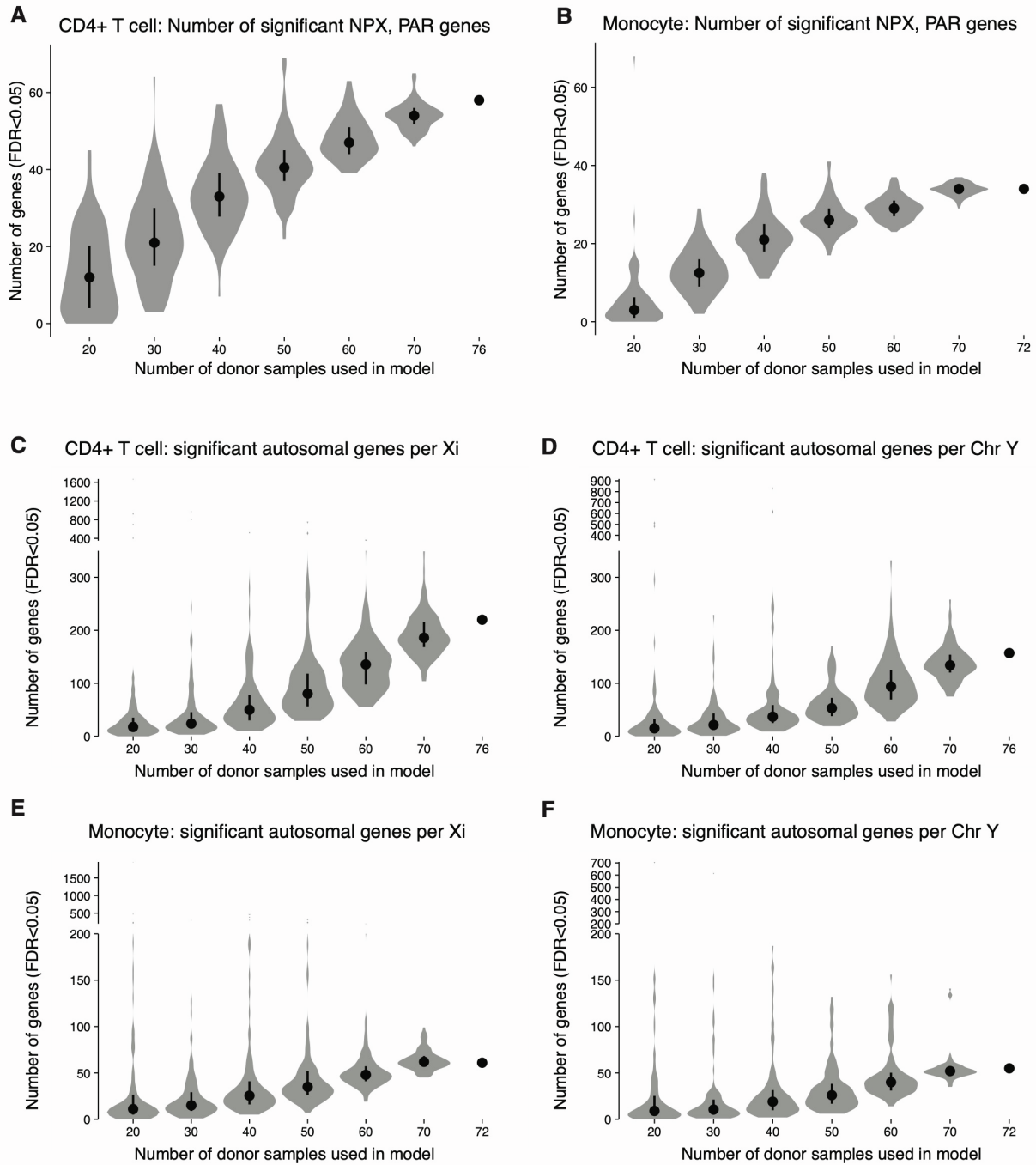


**Figure S5. Saturation analyses of detected significant gene responses to Xi or Chr Y dosage, related to Figure 2.**

Subsampling the full dataset demonstrates that the number of significantly responsive NPX and PAR genes (**A, B**) as well as the number of autosomal genes with significant responses to Xi (**C, E**) or Chr Y (**D, F**) dosage increase when more donor samples of CD4<sup>+</sup> T cells and monocytes are utilized in the linear models. Violin plots show distributions of numbers of significant genes in 100 subsampling experiments.

Figure S6

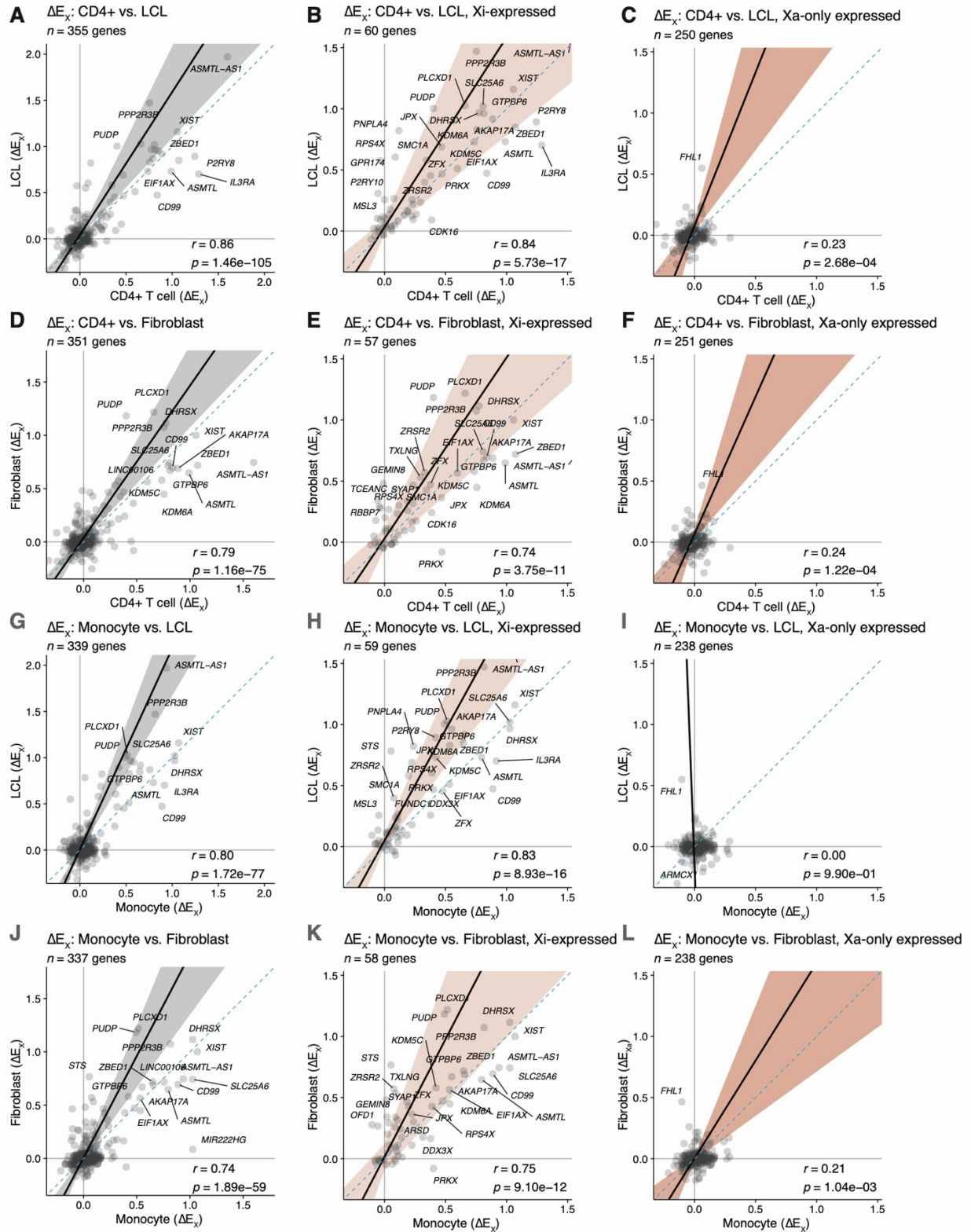


**Figure S6. X-chromosomal responses to Xi dosage are consistent across *in vivo* and *in vitro* cell types, gene-by-gene, related to Figure 2.**

(A - L) Scatter plots comparing  $\Delta E_X$  values for all NPX and PAR genes (A, D, G, J), genes expressed on Xi (B, E, H, K), or genes only expressed on Xa (C, F, I, L) between the indicated cell types. The plotted genes are expressed in both of the indicated cell types. Deming regression line in black with 95% confidence intervals shaded gray; blue dotted lines indicate X=Y identity line. Pearson correlation statistics are shown. Confidence intervals are not plotted for (I), as the intervals were broader than the plot axes.

**Figure S7**

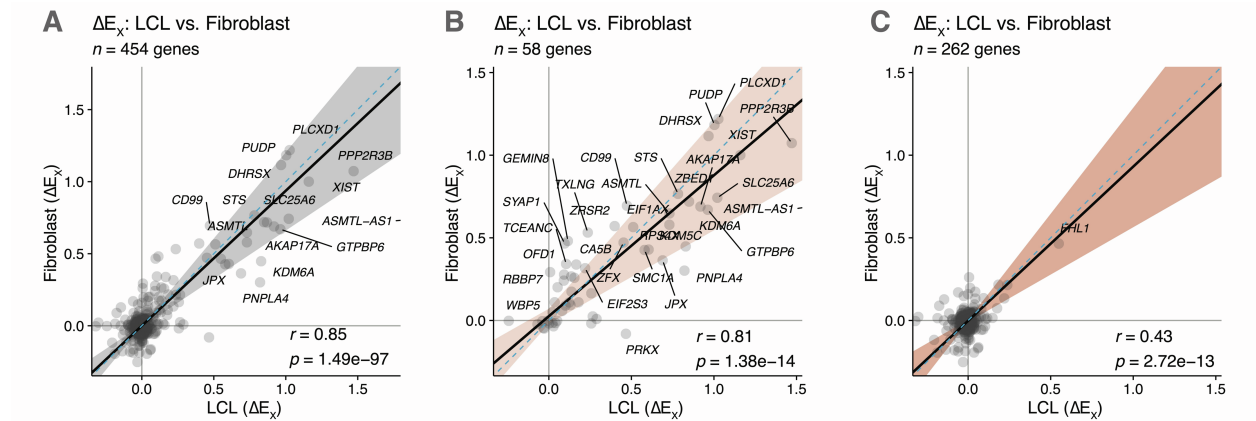


**Figure S7. X-chromosomal responses to Xi dosage are consistent across *in vitro* cell types, gene-by-gene, related to Figure 2.**

(A - C) Scatter plots comparing  $\Delta E_X$  values for all NPX and PAR genes (A), genes expressed on Xi, (B), or genes only expressed on Xa (C) between the indicated cell types. The plotted genes are expressed in both of the indicated cell types. Deming regression line in black with 95% confidence intervals shaded gray; blue dotted lines indicate X=Y identity line. Pearson correlation statistics are shown.

**Figure S8**

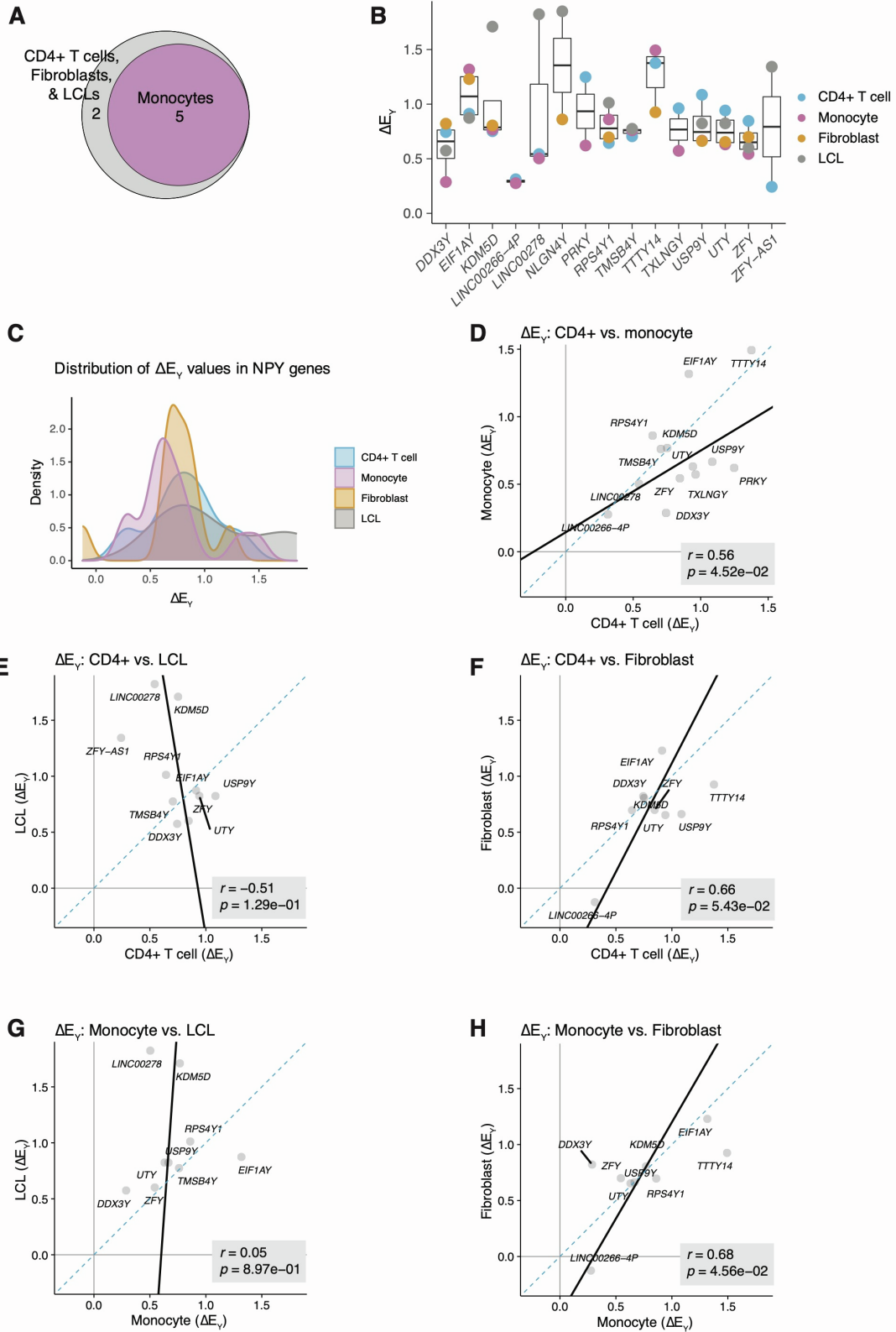


**Figure S8. NPY responses to Chr Y dosage across *in vitro* and *in vivo* cell types, related to Figure 2.**

(A) Venn diagram of NPY genes with statistically significant  $\Delta E_Y$  values across the four cell types. (B)  $\Delta E_Y$  values for each expressed NPY gene, colored by cell type; dots are only shown for genes expressed in the given cell type. (C) Density plot showing distribution of  $\Delta E_Y$  values across the four cell types. (D-H) Scatter plots comparing  $\Delta E_Y$  values between the indicated cell types. Deming regression line in black; blue dotted lines indicate X=Y identity line. Pearson correlation statistics are shown.



**Figure S9**

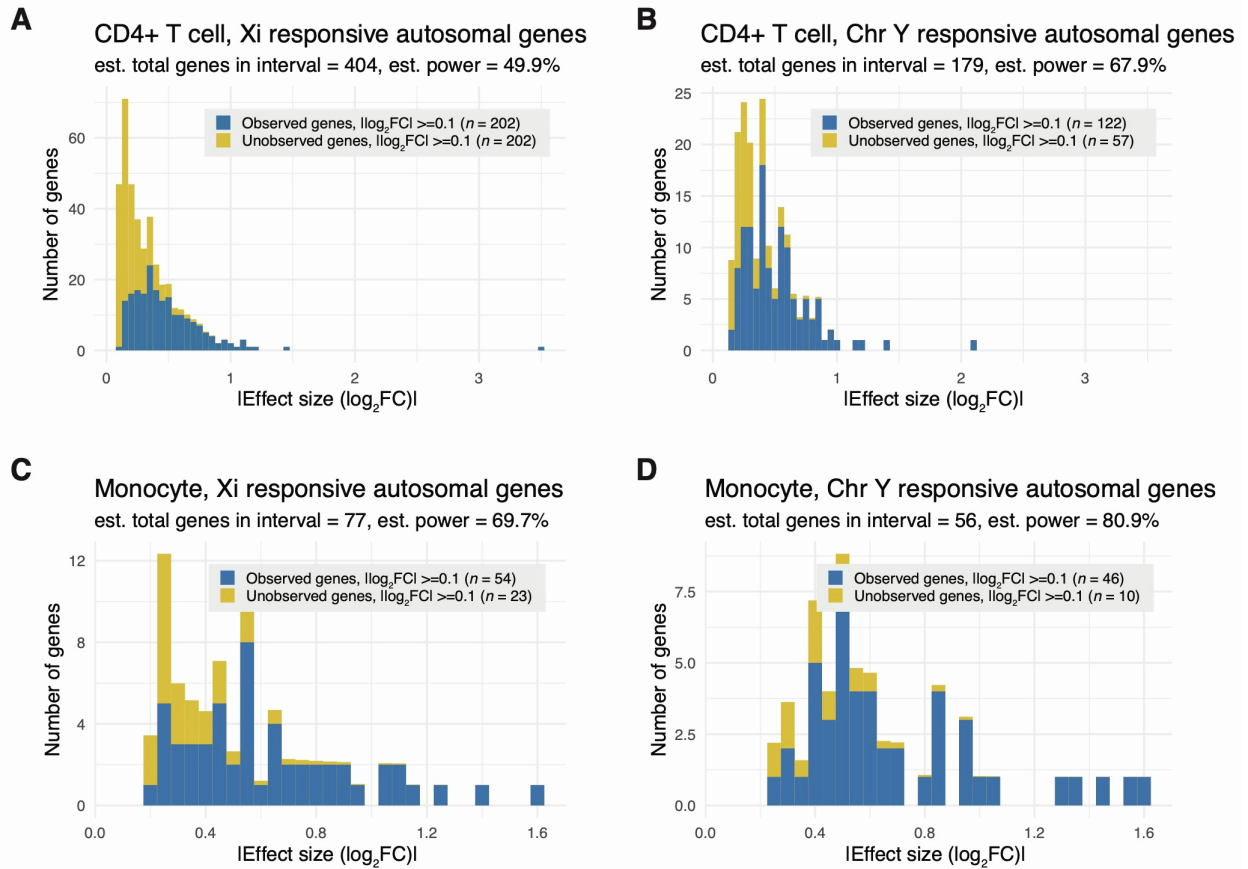
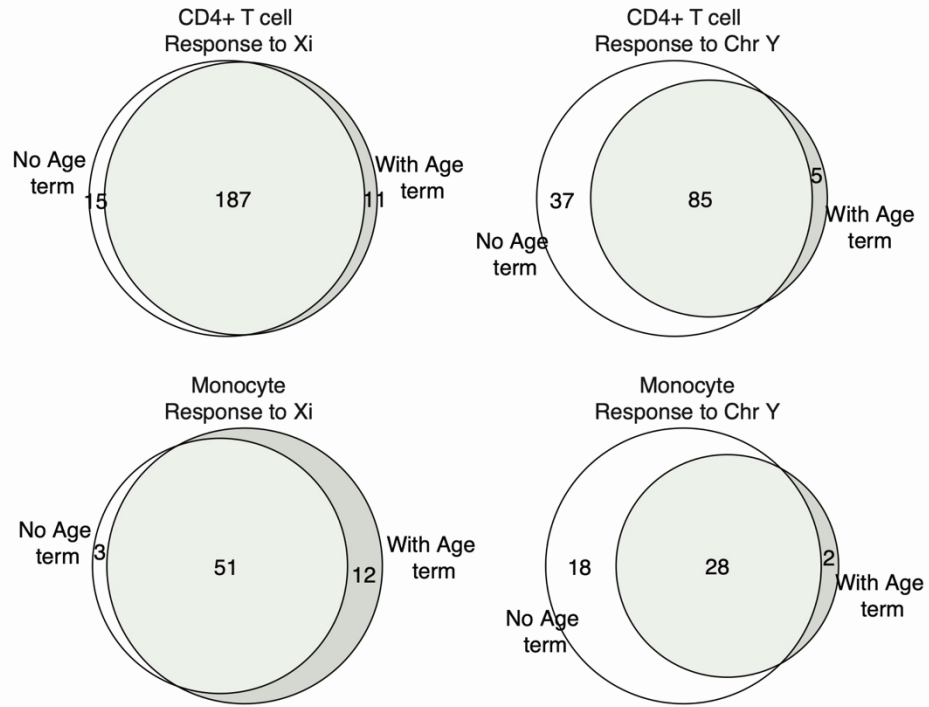


**Figure S9. Power analyses of observed and unobserved significant gene responses to Xi or Chr Y dosage in CD4+ T cells and monocytes, related to Figure 3.**

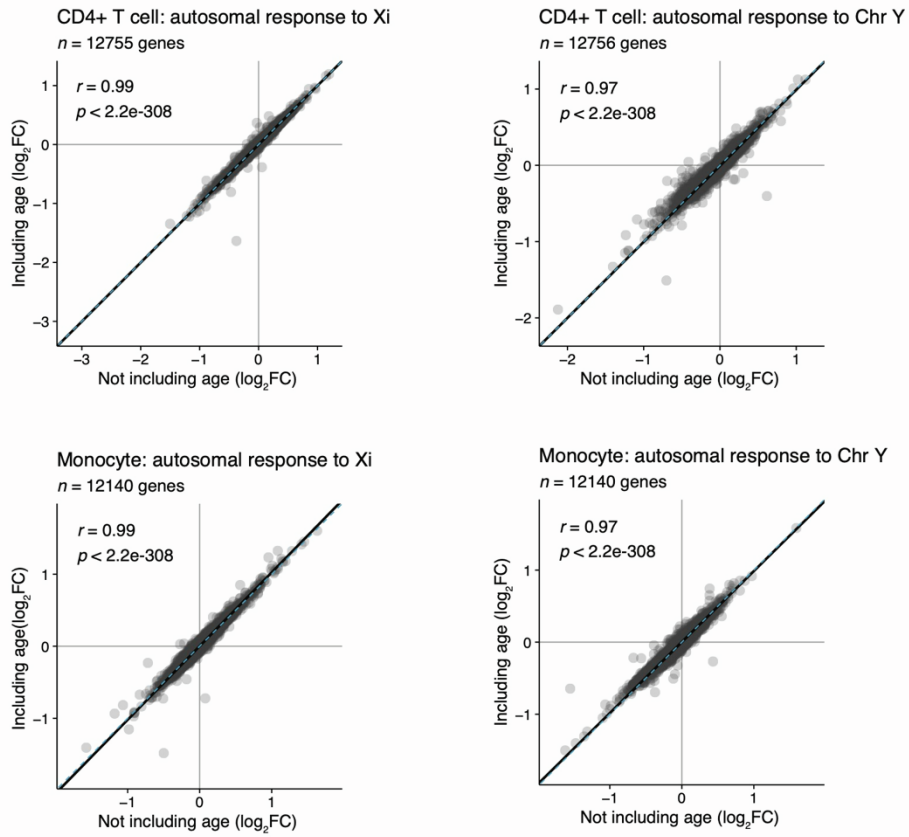
(A – D) Histograms depicting numbers of observed significantly responsive genes (in blue) and estimated unobserved significantly responsive genes (in yellow) by absolute effect size ( $|\log_2FC|$ ) for CD4+ T cells' response to Xi (A) and Chr Y (B) and monocytes' response to Xi (C) and Chr Y (D). Estimated numbers of unobserved genes were calculated via power analyses as described in Methods.

Figure S10

**A**



**B**



**Figure S10. Inclusion of age in linear model does not alter estimates of autosomal response to Xi or Chr Y dosage, related to Figure 3.**

(A) Venn diagrams representing the numbers of autosomal genes with significant responses to Xi or Chr Y dosage, as indicated, with or without inclusion of age as a variable in the linear model.

(B) Scatter plots of  $\log_2$  fold-changes per Xi or Chr Y, as indicated, in CD4<sup>+</sup> T cells and monocytes with or without inclusion of age as a variable in the linear model. Deming regression line in black with 95% confidence intervals shaded gray; blue dotted lines indicate X=Y identity line. Pearson correlation statistics are shown.

**Figure S11**

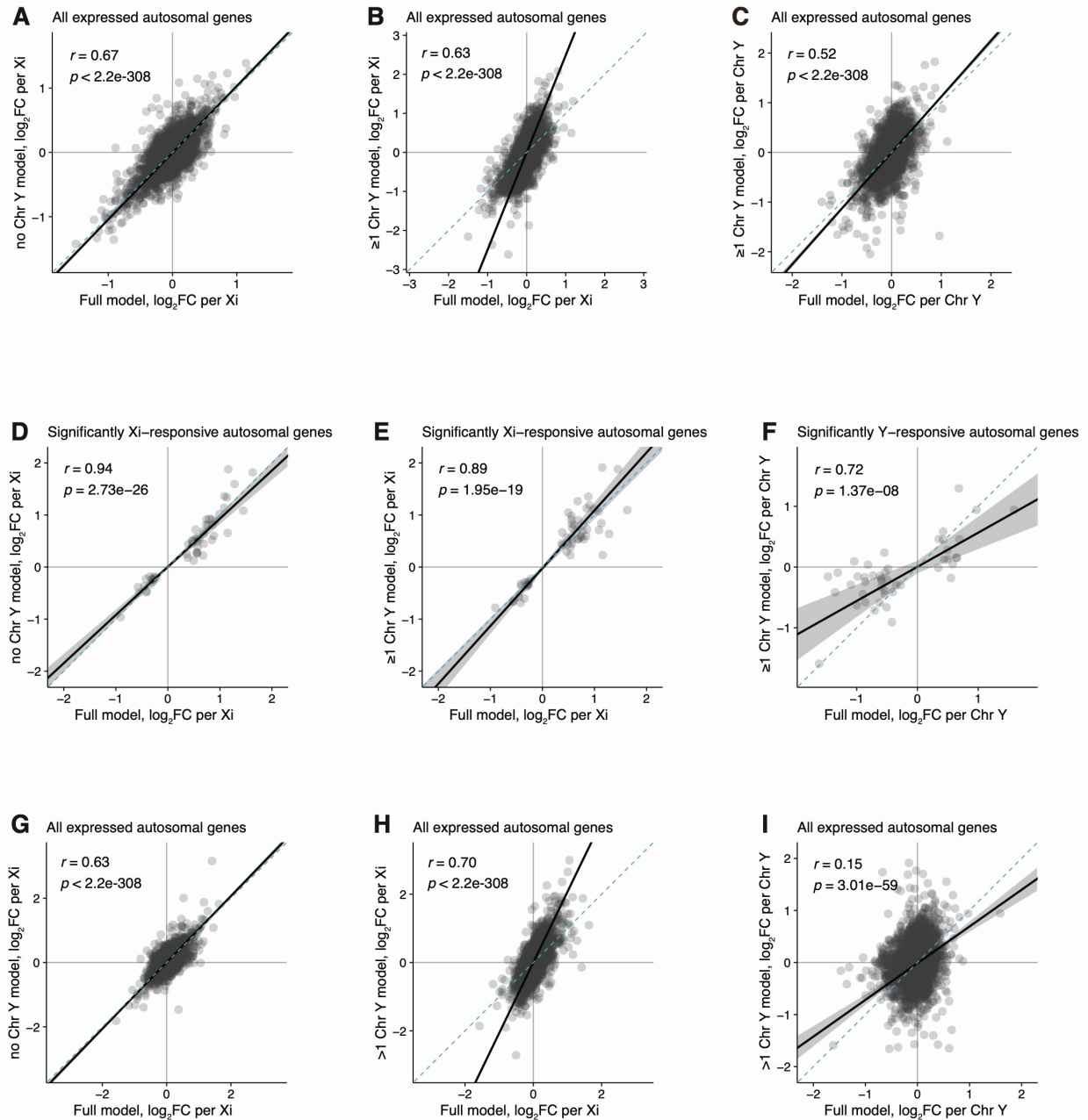


**Figure S11. Linear models built with no Chr Y or at least one Chr Y correlate with the full model containing all karyotypes, related to Figure 3.**

(A) Scatter plot of log<sub>2</sub> fold-changes per Xi for all expressed autosomal genes in CD4+ T cells, comparing effect sizes found in full model with all available karyotypes versus ‘no Chr Y’ subset

model. **(B, C)** Scatter plot of  $\log_2$  fold-changes per Xi **(B)** or Chr Y **(C)** for all expressed autosomal genes in CD4<sup>+</sup> T cells, comparing effect sizes from full model with all available karyotypes versus  $\log_2$  fold-changes in ‘ $\geq 1$  Chr Y’ subset model. **(D)** Scatter plot of  $\log_2$  fold-changes per Xi for genes with significant Xi response in monocytes, comparing effect sizes found in full model with all available karyotypes versus ‘no Chr Y’ subset model. **(E, F)** Scatter plot of  $\log_2$  fold-changes per Xi **(E)** or Chr Y **(F)** for significantly responsive autosomal genes in monocytes, comparing effect sizes from full model with all available karyotypes versus  $\log_2$  fold-changes in ‘ $\geq 1$  Chr Y’ subset model. **(G)** Scatter plot of  $\log_2$  fold-changes per Xi for all expressed autosomal genes in monocytes, comparing effect sizes found in full model with all available karyotypes versus ‘no Chr Y’ subset model. **(H, I)** Scatter plot of  $\log_2$  fold-changes per Xi **(H)** or Chr Y **(I)** for all expressed autosomal genes in monocytes, comparing effect sizes from full model with all available karyotypes versus  $\log_2$  fold-changes in ‘ $\geq 1$  Chr Y’ subset model. Deming regression line in black with 95% confidence intervals shaded gray; blue dotted lines indicate X=Y identity line. Pearson correlation statistics are shown.

Figure S12

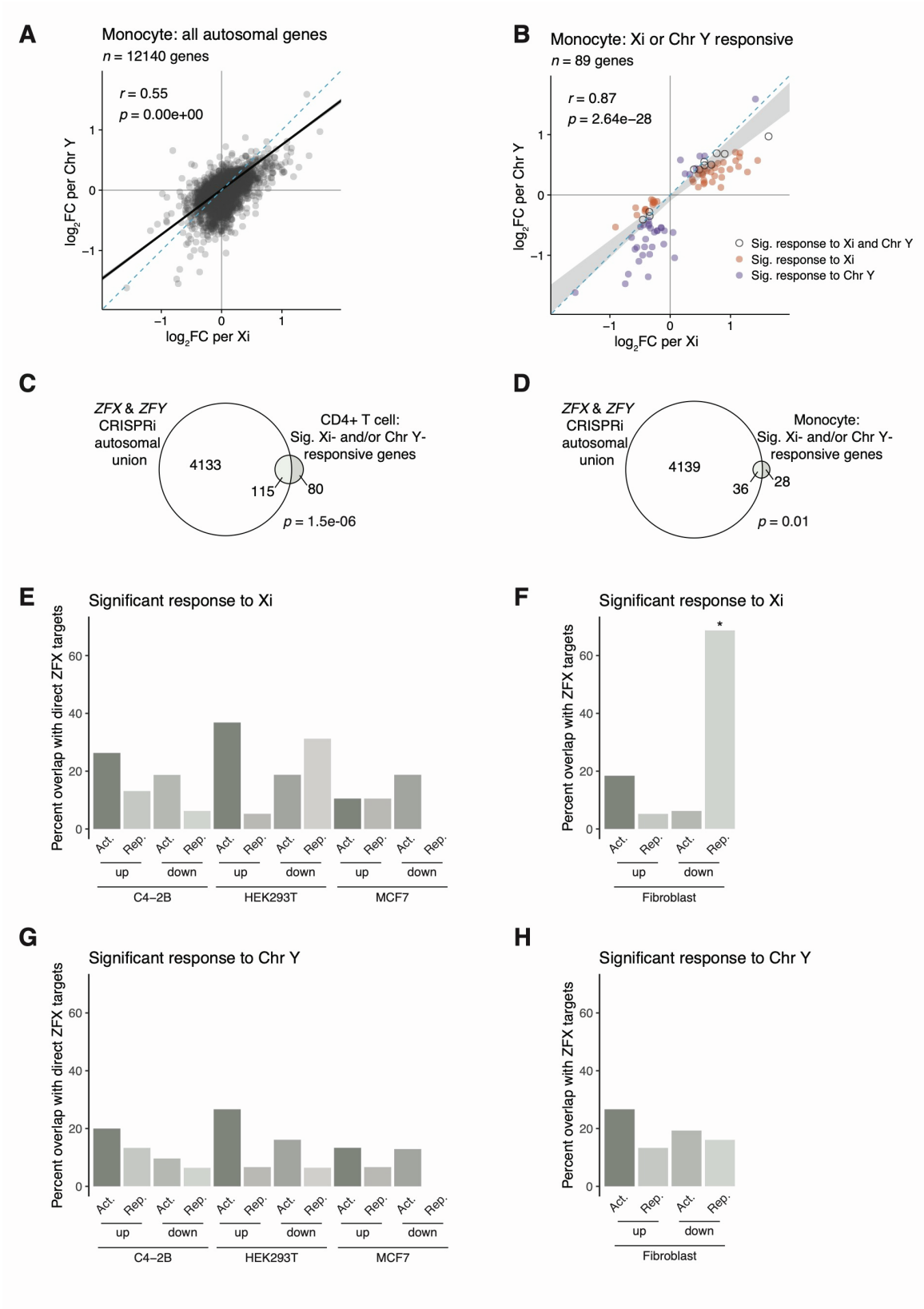


**Figure S12. ZFX and ZFY responsive genes explain a significant portion of the autosomal response to Xi dosage, related to Figure 4.**

(A, B) Scatter plot of  $\log_2$  fold-changes per Xi versus Chr Y dosage of all expressed autosomal genes in monocytes (A) or limited to genes significantly responsive to Xi (orange), Chr Y (purple), or both (gray) (B). (C, D) Venn diagrams displaying intersection of autosomal genes that respond to Xi or Chr Y in CD4<sup>+</sup> T cells (C) or monocytes (D) with genes that respond to ZFX or ZFY knockdown via CRISPRi in fibroblasts. Autosomal gene sets were restricted to genes expressed in both fibroblasts and CD4<sup>+</sup> T cells (C) or fibroblasts and monocytes (D). (E - H) Bar plots showing percentage of genes responsive to Xi and/or Chr Y dosage in monocytes that were identified as ZFX direct target genes in MCF7, C4-2B, and HEK-293T cell lines, or ZFX responsive in fibroblasts. Genes are parsed by whether they significantly increased or decreased with Xi or Chr Y dosage (“up” or “down”) and were activated or repressed by ZFX (“Act.” or “Rep.”). *p*-values reflect hypergeometric tests to identify significant enrichments of ZFX target genes in Chr X- or Y-responsive genes. Each comparison was restricted to genes expressed in both monocytes and the given *in vitro* cell line. Asterisks indicate the enrichment’s *p*-value was lower than the Bonferroni-adjusted threshold of 0.001.

**Figure S13**

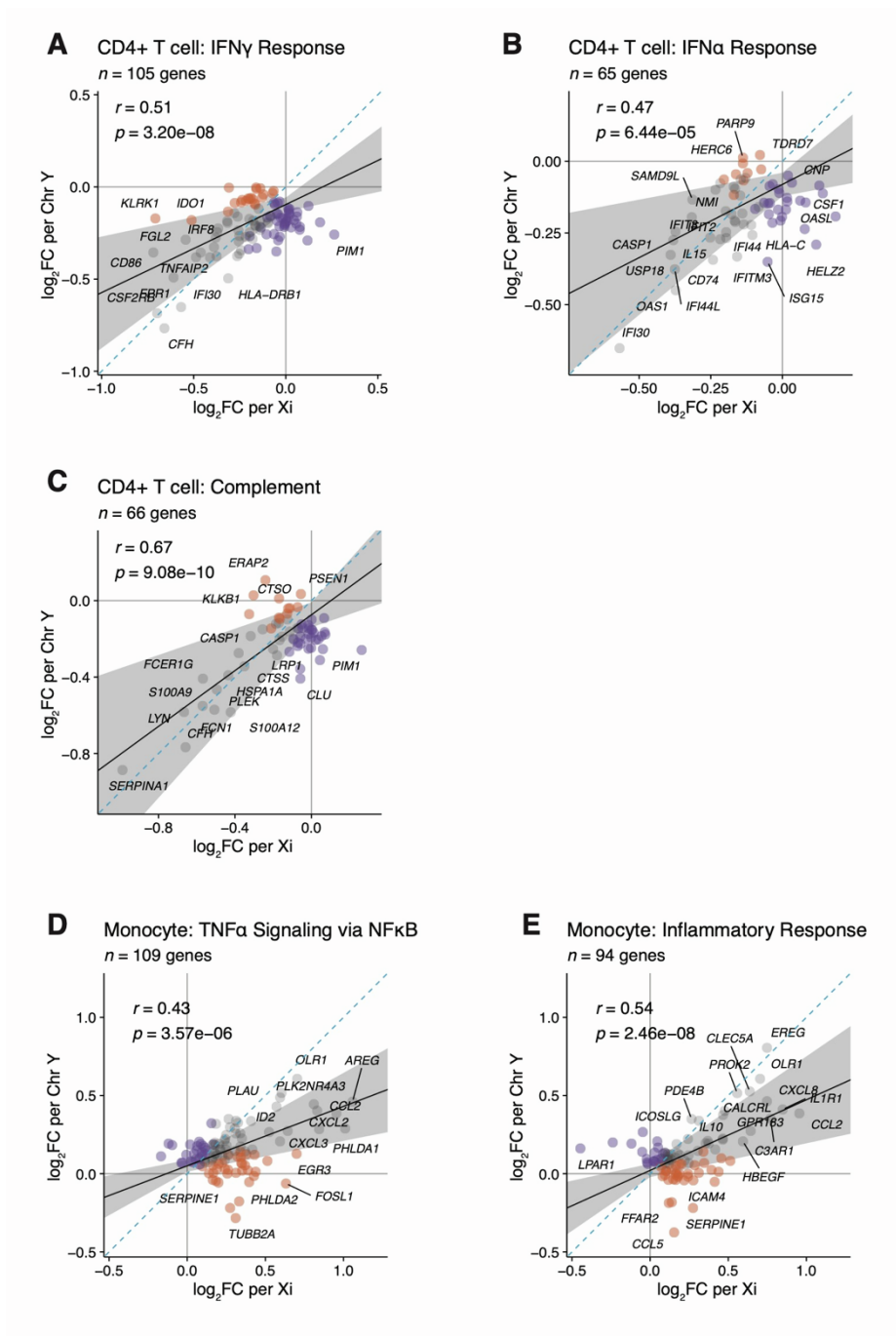


**Figure S13. Leading edge genes in significantly enriched gene sets respond similarly to Xi and Chr Y dosage, related to Figure 5.**



**(A-C)** Scatter plot of  $\log_2$  fold-changes per Xi versus Chr Y dosage of leading edge genes driving significant enrichments for the interferon gamma response pathway **(A)**, interferon alpha response pathway **(B)**, and complement **(C)** gene sets in CD4<sup>+</sup> T cells. **(D, E)** Scatter plot of  $\log_2$  fold-changes per Xi versus Chr Y dosage of leading edge genes driving significant enrichments for the TNF $\alpha$  signaling via NF $\kappa$ B **(D)** and inflammatory response **(E)** gene sets in monocytes. The plotted genes are leading edge genes from the Chr X model (orange), Chr Y model (purple) or both (gray). Deming regression line in black with 95% confidence intervals shaded gray; blue dotted lines indicate X=Y identity line. Pearson correlation statistics are shown.

**Figure S14**

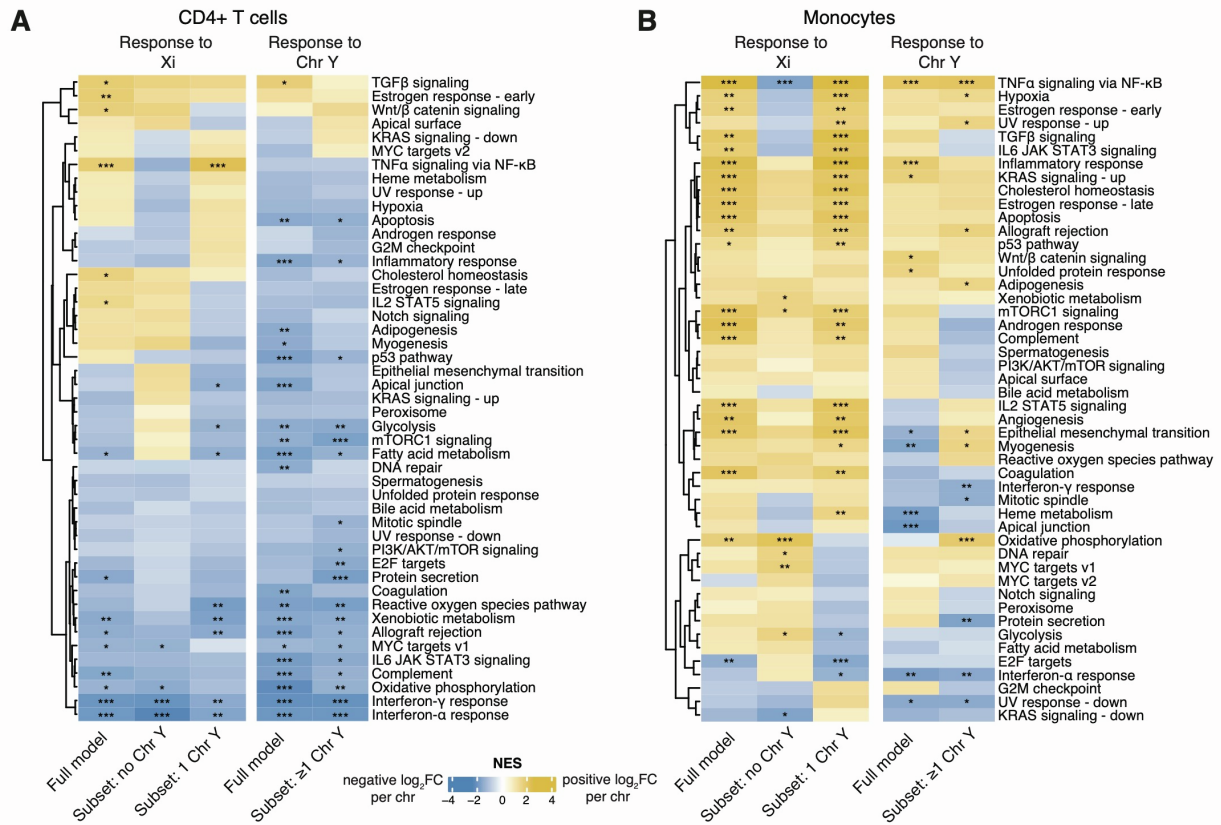


**Figure S14. CD4+ T cell functional enrichments remain largely consistent regardless of the presence or absence of Chr Y, related to Figure 5.**

(A, B) Heatmaps of normalized enrichment scores (NES) from gene set enrichment analysis with Hallmark gene sets in CD4+ T cells (A) and monocytes (B) for either the full models or subset models as indicated; significant enrichments indicated by asterisks (\* =  $p\text{-adj} < 0.05$ ; \*\* =  $p\text{-adj} < 0.01$ ; \*\*\* =  $p\text{-adj} < 0.001$ ).

Figure S15

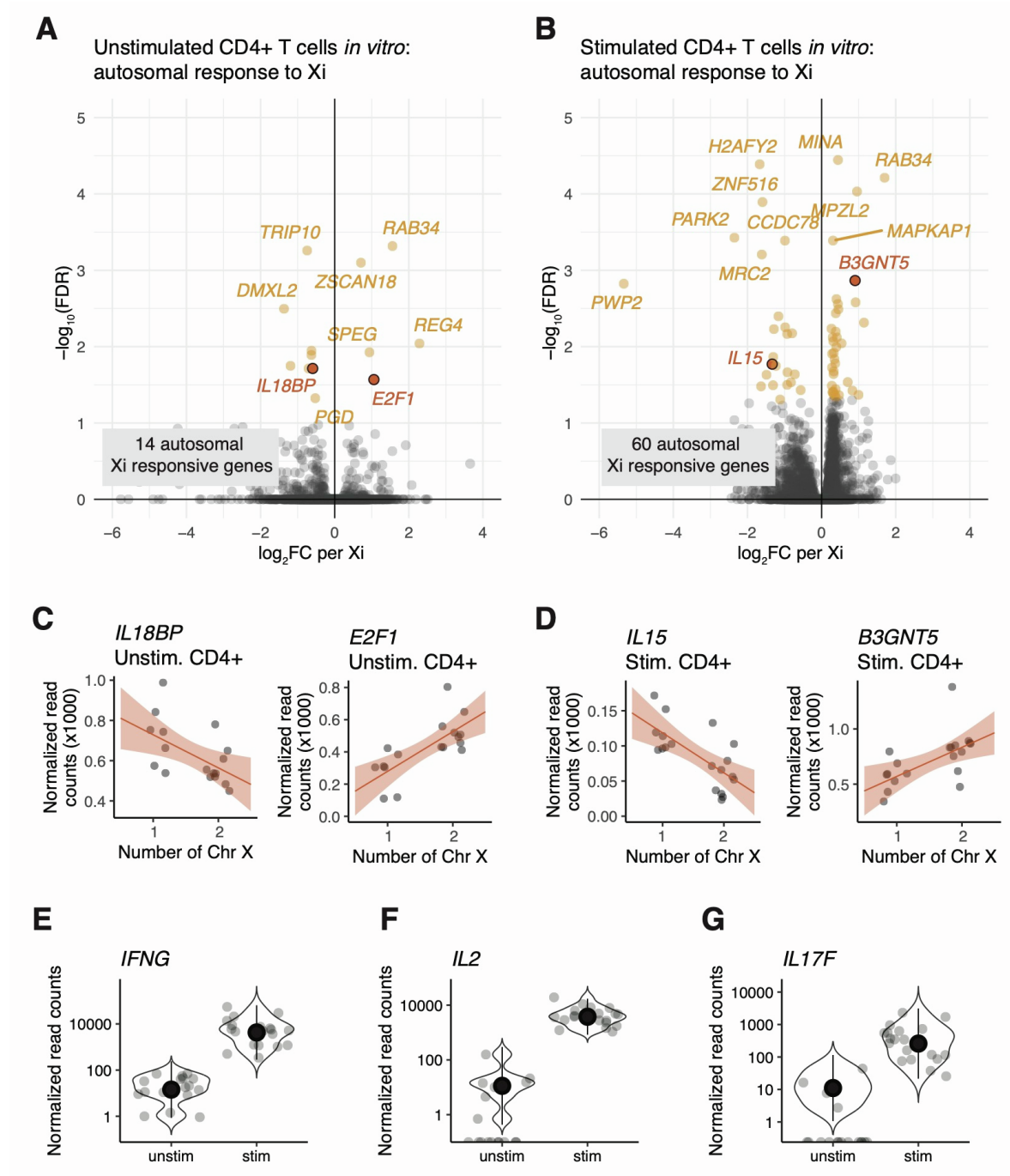
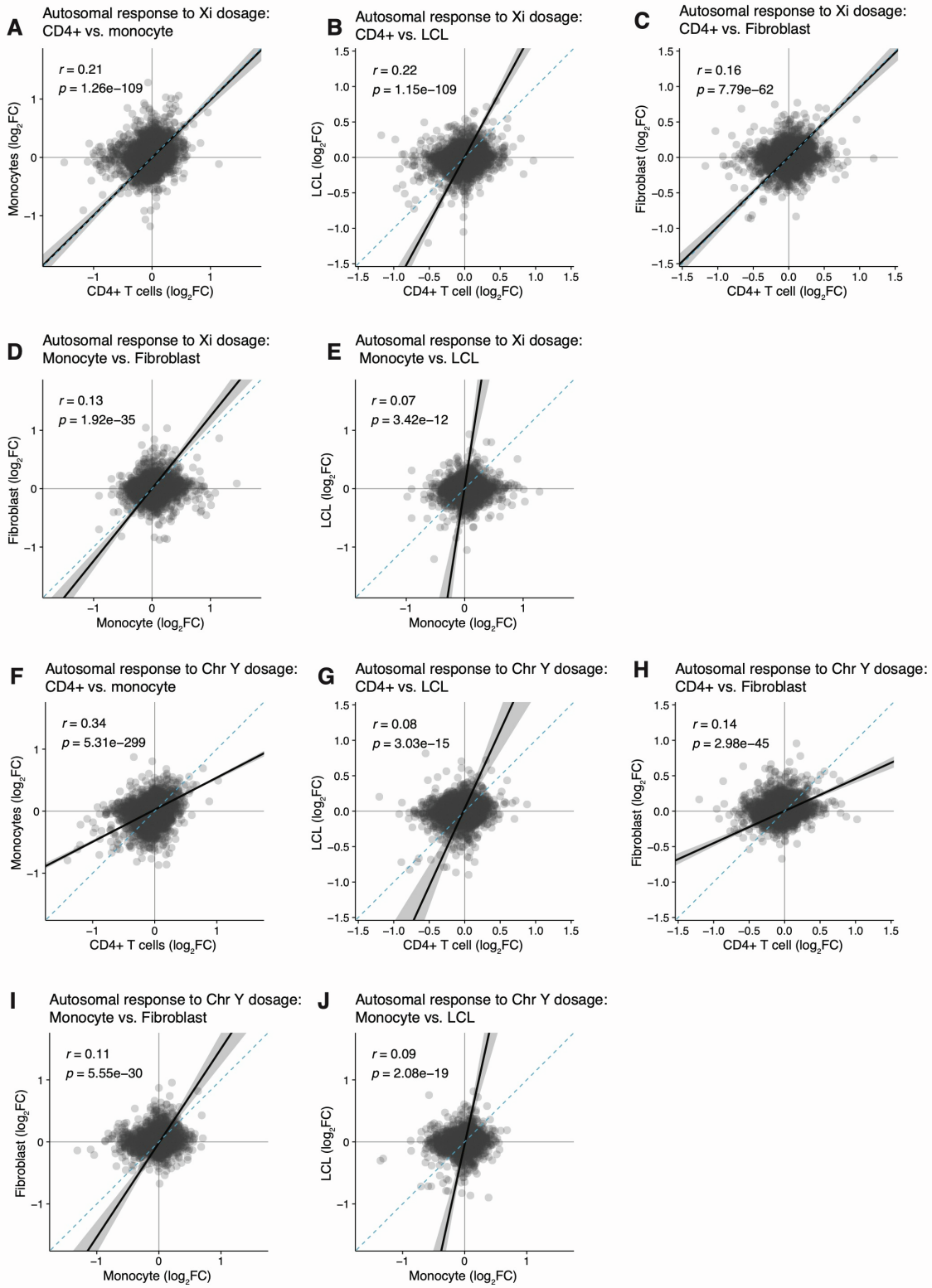


Figure S15. Xi dosage has significant effects on CD4+ T cell activation, related to Figure 5.

(A, B) Volcano plots of autosomal responses to Xi dosage for *in vitro* unstimulated CD4+ T cells (five positively and nine negatively responsive genes) (A) and *in vitro* stimulated CD4+ T cells

(37 positively and 23 negatively responsive genes) **(B)**. **(C, D)** Examples of positively and negatively Xi responsive genes in unstimulated CD4<sup>+</sup> T cells **(C)** or stimulated CD4<sup>+</sup> T cells **(D)**. Regression lines with confidence intervals are shown. **(E-G)** Normalized read counts showing increased *IFNG*, *IL2*, and *IL17F* gene expression with the addition of T cell activation beads, indicating that CD4<sup>+</sup> T cell activation was successful.

Figure S16



**Figure S16. Autosomal responses to Xi dosage are cell-type-specific, related to Figure 6.**

**(A – E)** Scatter plots of  $\log_2$  fold-changes for all expressed autosomal genes in response to Xi dosage between the indicated cell types. Deming regressions (solid black line with 95% confidence intervals shaded gray) and Pearson correlation statistics are shown. **(F – J)** Scatter plots of  $\log_2$  fold-changes for all expressed autosomal genes in response to Chr Y dosage between the indicated cell types. Deming regression line in black with 95% confidence intervals shaded gray; blue dotted lines indicate X=Y identity line. Pearson correlation statistics are shown.